This reaction went to completion because $Ru_3(CO)_{12}$ sublimed from the system at 80 °C. Equilibrium experiments at 60 °C are described below.

X. Tetranuclear/Trinuclear Cluster Equilibrium Studies. A. Reaction of $[HRu_3(CO)_{11}]^-$ with $Ru_3(CO)_{12}$. In the drybox, 78.8 mg (0.121 mmol) of $K[HRu_3(CO)_{11}]$ and 26.0 (0.0407 mmol) of $Ru_3(CO)_{12}$ were weighed into a 50-mL reaction vessel. Glyme, 4 mL, was distilled onto the reactants at -78 °C, and the system was warmed to 80 °C. Noncondensible gases were removed from time to time as the reaction progressed. After 4 h, 0.24 mmol of CO gas had been evolved and a ^1H NMR spectrum of the reaction solution showed only $K[HRu_4(CO)_{13}]$. An infrared spectrum confirmed that $K[HRu_4(CO)_{13}]$ had been formed and $K[HRu_3(CO)_{11}]$ and $Ru_3(CO)_{12}$ had been completely consumed.

B. Reaction of $K[HRu_3(CO)_{11}]$ with $Ru_3(CO)_{12}$ under H_2. In the drybox, 45.0 mg (0.069 mmol) of $K[HRu_3(CO)_{11}]$ and 15.0 mg (0.023 mmol) of $Ru_3(CO)_{12}$ were weighed into a 100-mL reaction vessel. Glyme, 3 mL was distilled into the vessel at -78 °C and H_2 (1 atm), was expanded over the solution. Stirring at 80 °C resulted in quantitative formation of $K[H_3Ru_4(CO)_{12}]$ after 16 h as evidenced by ^1H NMR. Mass spectral analysis of the gas over the solution indicated that CO had been evolved (~0.14 mmol).

C. Reaction of $[H_3Ru_4(CO)_{12}]^-$ with CO/H_2 Mixtures. The reaction of $K[H_3Ru_4(CO)_{12}]$ with CO/H_2 mixtures was performed in a 120-mL reaction vessel at 60 °C under a total gas pressure of 1 atm. The species present in solution were determined by ^1H NMR spectroscopy taken as a function of time. In the drybox, 91.5 mg (0.117 mmol) of $K[H_3Ru_4(CO)_{12}]$ was weighed into the reaction vessel adapted with a NMR tube as a sidearm. Glyme, 3 mL, was condensed onto the solid at -78 °C and a CO/H_2 mixture of known composition was expanded over the solution. The reaction vessel was stirred at 60 °C for at least 24-h periods and the gas above the solution was analyzed by mass spectrometry. Proton NMR spectra of the reaction solution were recorded under the CO/H_2 atmosphere. This process was repeated to ensure that equilibrium had been achieved during the time frame of the experiment. The results are given in Table II for reaction in glyme. Similar results were obtained in THF and ethoxyethanol. The equilibrium was tested by also examining the reverse reaction, starting with a 3:1 ratio of $[HRu_3(CO)_{11}]^-$:$Ru_3(CO)_{12}$ under CO/H_2 mixtures as described below.

D. Reaction of $[HRu_3(CO)_{11}]$:$Ru_3(CO)_{12}$ (3:1) with CO/H_2 Mixtures. The reaction of a 3:1 mixture of $K[HRu_3(CO)_{11}]$:$Ru_3(CO)_{12}$ with CO/H_2 mixtures was performed identically with those of $K[H_3Ru_4(CO)_{12}]$ as described above. For the experiments performed in this manner, 75.1 mg (0.117 mmol) of $K[HRu_3(CO)_{11}]$ and 24.9 mg (0.039 mmol) of $Ru_3(CO)_{12}$ were employed. Results are given in Table II. Irrespective of the starting point, the same ratio of $[H_3Ru_4(CO)_{12}]^-$ to $[HRu_3(CO)_{11}]^-$ was achieved at a given CO/H_2 ratio.

Acknowledgment. This work was supported by the National Science Foundation through Grant No. CHE 79-18148. J.C.B. thanks the Ohio State University for a Presidential Fellowship. We would like to thank Professor R. F. Firestone for the use of the Pd thimble.

Examination of Rhodium Carboxylate Antitumor Agents Complexed with Nucleosides by Extended X-ray Absorption Fine Structure Spectroscopy

N. Alberding,*† N. Farrell,‡ and E. D. Crozier†

Contribution from the Department of Physics, Simon Fraser University, Burnaby, B.C., Canada V5A 1S6, and Universidade Federal de Minas Gerais, Instituto de Ciências Exatas, 30000 Belo Horizonte, MG, Brazil. *Received April 3, 1984*

Abstract: Extended X-ray absorption fine structure spectra have been measured of rhodium carboxylates and their complexes with five adenine nucleoside systems in order to elucidate the structural basis of the antineoplastic activity of such complexes. The analysis reveals several structural features. The Rh-Rh bond lengths of $[Rh_2Ac_4(adenosine)]\cdot H_2O$, $[Rh_2Ac_4(cordycepin)]\cdot H_2O$, $[Rh_2Ac_4(ara\text{-}A)]\cdot H_2O$, and $[Rh_2Ac_4(8\text{-}Br\text{-}adenosine)]\cdot H_2O$ are the same, within experimental uncertainty, as that of $[Rh_2Ac_4(caffeine)_2]$, 2.395 Å (Ac is used for acetate rather than acetyl). The Rh-Rh bond length of $[Rh_2Bu_4\cdot 2MeOH]$, however, is 0.026 Å shorter than in the rhodium acetate complexes. Substituting 8-bromoadenosine in $[Rh_2Ac_4(adenosine)]$ results in a significant change in the disorder parameters of the first coordination shell around Rh. Furthermore, the complexation of rhodium acetate to 8-bromoadenosine elicits a syn to anti conformation change at the nucleoside. It is concluded that rhodium probably binds the purine at N_7 in the adenosine complex and at N_1 in the 8-bromoadenosine complex.

The interaction of metal complexes with nucleic acids is of current interest.[1,2] We report here structural studies on rhodium carboxylate adenine nucleoside systems by extended X-ray absorption fine structure (EXAFS) spectroscopy. These species are active antitumor agents[3,4] and bind specifically to adenine and its nucleotides and nucleosides.[5]

The factors which affect specificity in metal-purine binding are now well delineated[6,7] and of particular interest is the dictation of this specificity in the absence or presence of intramolecular hydrogen bonding between exocyclic groups and ligand donor atoms.[8]

The binding site of purines to rhodium carboxylates has been assigned to N_7, due to favorable H-bonding interaction between the exocyclic amino group and the acetate oxygens of the ligands,[9,10] by analogy with the structure elucidated for $[Co(acac)_2(NO_2)](2'\text{-deoxyadenosine})$.[3] While the exact mechanism of action of the rhodium carboxylates is not clear,[11] rhodium-purine binding may still be important. Thus, the possibility that

† Simon Fraser University.
‡ Universidade Federal de Minas Gerais. Present address: Department of Chemistry, University of Vermont, Burlington, Vermont.

(1) Hodgson, D. G. *Prog. Inorg. Chem.* **1977**, *23*, 211.
(2) Marzilli, L. G. *Prog. Inorg. Chem.* **1977**, *23*, 255.
(3) Bear, J. L.; Gray, H. B., Jr.; Rainen, L.; Chang, I. M.; Howard, R.; Serio, G.; Kimball, A. P. *Cancer Chemother. Rep.* **1975**, *59*, 611.
(4) Hughes, R. G.; Bear, J. L.; Kimball, A. P. *Proc. Am. Assoc. Cancer Res.* **1972**, *13*, 120.
(5) Rainen, L.; Howard, R. A.; Kimball, A. P.;Bear, J. L. *Inorg. Chem.* **1975**, *14*, 2752.
(6) Martin, R. B.; Mariam, Y. H. *Met. Ions Biol. Syst.* **1979**, *8*, 57.
(7) Marzilli, L. G. *Adv. Inorg. Biochem.* **1981**, *3*, 47.
(8) Marzilli, L. G.; Kistenmacher, T. J. *Acc. Chem. Res.* **1977**, *10*, 146.
(9) Farrell, N. *J. Inorg. Biochem.* **1981**, *14*, 261.
(10) Aoki, K.; Yamazaki, H. *J. Chem. Soc., Chem. Commun.* **1980**, 186.
(11) Howard, R. M.; Spring, T. G.; Bed, J. L. *Cancer Res.* **1976**, *36*, 4402.

0002-7863/85/1507-0384$01.50/0 © 1985 American Chemical Society

this activity is directly affected by a chemical factor such as H-bonding is further reason for an unequivocal picture of the structure of these complexes.

Concurrent with this emphasis on metal–purine chemistry, the fundamental role of purines and pyrimidines in cellular metabolism is such that a wide variety of analogue inhibitors,[10] both synthetic and naturally occurring, have been employed as chemotherapeutic agents. Two classes may be distinguished: those based on alterations in the purine and pyrimidine rings and those based on changes in the sugar (nucleoside) moiety. The presence of the adenine ring in antibiotics such as cordycepin (3′-deoxyadenosine) (II) and ara-A (9-β-arabinofuranosyladenine) (III) prompted us

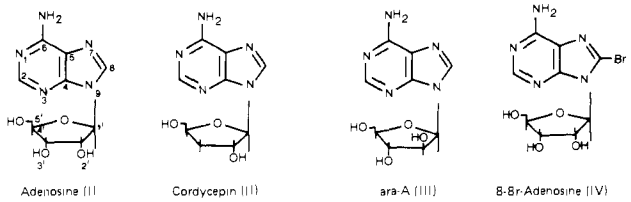

to undertake a survey of the chemical and biological properties of their metal complexes and it was reasonable for the reasons outlined above to begin with the rhodium carboxylates.

The use and potential of EXAFS spectroscopy in the elucidation of bioinorganic structures have been extensively studied in the last years[12] and applications with metal–DNA and metal–purine complexes have been made.[13-16] Very few X-ray crystal structures are known for metal–nucleoside complexes because they are notoriously difficult to crystallize. EXAFS spectroscopy can render structural information on many of these complexes which defy analysis by X-ray crystallography and thus it is of some interest to extend its use to the present system. The present paper presents EXAFS results on rhodium acetate complexes of I–IV, caffeine, and $Rh_2(Bu)_4 \cdot 2MeOH$ (Bu = butyrate).

Experimental Section

The new complexes of I–IV with rhodium acetate were prepared by previously reported methods[9] and precipitated from aqueous solution as pink solids. Elemental analyses were satisfactory for 1:1 adducts.

Absorption spectra were recorded on powdered samples which had been packed into holes, 1.9 mm in diameter and 1.7 mm thick, in a Plexiglas sheet then masked with lead. Beam line IV-1 at the Stanford Synchrotron Radiation Laboratory was used with a Si(220) double-crystal monochromator. The monochromator crystals were detuned to reduce harmonic content. The intensities of the X-ray beam before the sample, I_0, and after the sample, I, were measured with ionization chambers. The absorption spectrum $\mu = \ln (I/I_0)$ as a function of the X-ray photon energy $E = h\nu$ was obtained by tuning the monochromator from 200 eV below the Rh and Br absorption edges to the maximum energy.

The low-temperature spectra were recorded by using a liquid nitrogen-cooled cold finger placed in a foam-insulated cryostat. A temperature of −185 °C was attained. In all cases three or four spectra were recorded sequentially and then averaged before analysis.

Analysis

The extended X-ray absorption fine structure spectrum is derived from the absorption spectrum above the Rh absorption edge, E_0 = 23 205 eV, and the Br edge, E_0 = 13 385 eV. $\mu(k)$ is the absorption coefficient as a function of k, the photoelectron wave vector defined as

$$k = \left[\frac{2m_e}{\hbar^2}(E - E_0)\right]^{1/2}$$

The edge energy was set at the inflection point of the absorption edge step. If μ_0 is the free atom absorption cross section, μ_{BG} is the background absorption including μ_0 as well as other contributions to the experimental base line, then the EXAFS interference function is

$$\chi(k) = [\mu(k) - \mu_{BG}(k)]/\mu_0(k)$$

This function contains structural information about near neighbors of the absorbing atom. Its theoretical expression for the case of single scattering is[17]

$$\chi(k) = \sum_i \frac{A_i(k)e^{-r_i/\lambda}}{kr_i^2} \exp(-2\sigma_i^2k^2)|f_i(k,\pi)| \sin [2kr_i + \alpha_i(k)] \quad (1)$$

where r_i is the mean distance from the X-ray absorbing atom to the ith backscattering atom. α_i is the phase shift characteristic of the central-backscattering atom pair. $|f_i(k,\pi)|$ is the modulus of the backscattering amplitude. The factor $\exp(-2\sigma_i^2k^2)$ results from static or dynamic deviations from r_i of atom i assuming a Gaussian distribution with standard deviation σ_i. λ is the photoelectron mean free path. The factor $A_i(k)$ describes effects of multiple scattering, shake-up, shake-off, and non-Gaussian pair distribution functions.[18] This factor we set to unity because these effects are not pertinent to the analysis of the present system. The single scattering formalism has proved satisfactory for analyzing the first coordination sphere environment of many systems. The bridging geometry of the Rh atoms by the carboxylate groups is too oblique for multiple scattering to be significant.[19]

The k-dependence of $|f(k,\pi)|$ is characteristic of the type of backscattering atom. Light atoms such as nitrogen have an $|f(k,\pi)|$ that is large at small k, and decays roughly exponentially with k. The Rh backscattering function, while also decaying with k between 4 and 7 Å^{-1}, again increases with k to peak at 10 Å^{-1} before finally decreasing. Thus when the spectrum is produced by a composite of N, C, O, and Rh backscattering, at low k all atoms contribute to the spectrum, whereas at high k only Rh backscattering contributes.

Results

Rh Edge Spectra. The EXAFS spectra from the Rh edge and their Fourier transforms are shown in Figure 1. The structural parameters obtained from the spectra are the rhodium–rhodium and rhodium–oxygen bond lengths r(Rh–Rh) and r(Rh–O) and the disorder parameters σ^2(Rh–Rh) and σ^2(Rh–O) representing the mean square deviations of these bond lengths from their central value. Values for the axial nitrogen or oxygen ligand could not be obtained as is discussed below. Curve fitting was used for the determinations; however, r(Rh–Rh) could also be determined by a simpler phase analysis at large k. This latter method was possible because Rh backscattering dominates that of light atoms (O, N, or C) above 8 Å^{-1}.

For the *phase analysis* the phase of the EXAFS is derived from the data by a Fourier filtering method.[20] From eq 1 the phase for the Rh shell is

$$\phi(k) = 2kr + \alpha(k)$$

The problem posed by the phase shift $\alpha(k)$ is bypassed if the distances in the unknown system are determined relative to that of a similar system in which the distance is known. We have chosen $Rh_2(O_2CCH_3)_4(caffeine)_2$ of known crystal structure[10] as the standard. Provided $\alpha(k)$ and E_0 are the same for the unknown and the standard, then

$$\Delta\phi = 2k(r_{Rh} - r_{standard}) \quad (2)$$

(12) Teo, B. K. *Acc. Chem. Res.* **1980**, *13*, 412.
(13) Teo, B. K.; Kizima, K.; Bau, R. *J. Am. Chem. Soc.* **1978**, *100*, 621.
(14) Teo, B. K.; Eisenberger, P.; Reed, J.; Barton, J. K.; Lippard, S. J. *J. Am. Chem. Soc.* **1978**, *100*, 3225.
(15) Hitchcock, A. P.; Lock, C. J. L.; Pratt, W. M. C. *Inorg. Chim. Acta* **1982**, *66*, L45.
(16) Bruck, M. A.; Korte, H.-G.; Bau, R.; Nadjiliadis, N.; Teo, B. K. *ACS Symp. Ser. No.* **1983**, *No. 209*, 245.
(17) Stern, E. A. *Phys. Rev. B* **1977**, *15*, 2862.
(18) (a) Stern, E. A.; Bunker, B. A.; Herald, S. M. *Phys. Rev. B* **1980**, *21*, 5521. (b) Crozier, E. D.; Seary, A. J. *Can. J. Phys.* **1980**, *58*, 1388.
(19) (a) Alberding, N.; Crozier, E. D.; *Phys. Rev. B* **1983**, *27*, 3374. (b) Teo, B. K. *J. Am. Chem. Soc.* **1981**, *103*, 3990–4001. (c) Boland, J. J.; Crane, S. E.; Baldeschwieler, J. D. *J. Chem. Phys.* **1982**, *77*, 142–153.
(20) Eisenberger, P.; Shulman, R. G.; Ogawa, S. *Nature (London)* **1978**, *274*, 30–34.

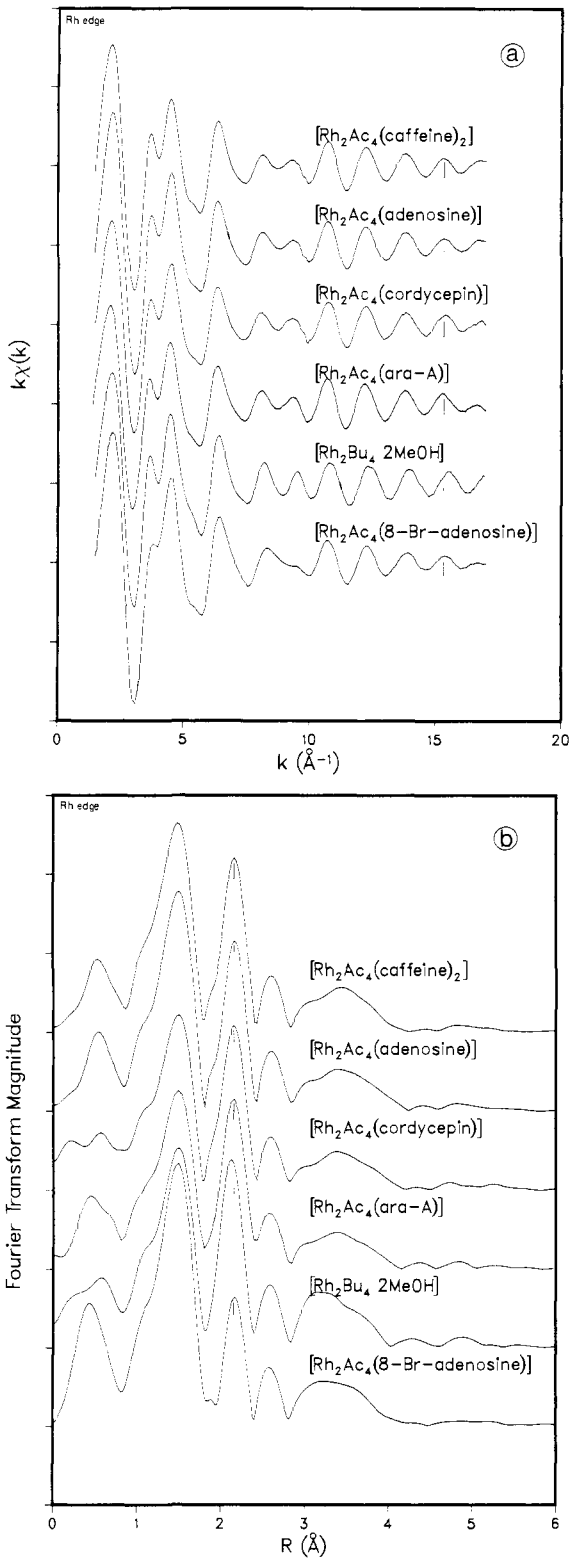

Figure 1. (a) EXAFS spectra of the Rh edge of six rhodium carboxylate compounds. The tick marks on each spectrum are at the same k value and show the phase shift of $[Rh_2Bu_4 \cdot 2MeOH]$ relative to the others. (b) Fourier transforms of the spectra of part a. The tick marks are at the same R value and show the displacement of the Rh peak in $[Rh_2Bu_4 \cdot 2MeOH]$ resulting from a 0.026-Å decrease in r(Rh–Rh). Transform is of $k\chi(k)$ over a range of 1.5–16 $Å^{-1}$ with a 10% Gaussian window applied. The peak positions in all Fourier transforms are less than the actual radial distances because of the phase shift $\alpha(k)$.

The lack of chemical differences (oxidation state, ligation) at the Rh site between the unknown and standard implies that the threshold energy E_0 is the same. As the data were analyzed in the range 9–17 $Å^{-1}$, the effect of E_0 changes is insignificant. Such an assumption is also borne out by the invariance of the observed edge inflection points and shape of the edge spectra. For the same reasons, the $\alpha(k)$'s should be equivalent.

Another possible cause for breakdown of transferability of $\alpha(k)$ between the standard to unknown is multiple scattering around the bridging geometry. Where a multiple scattering and direct backscattering interfere, a small structural deviation can severely perturb $\alpha(k)$. In the bridged rhodium carboxylates, the multiple scattering path Rh–O–C–O–Rh is so much longer than the Rh–Rh path that its interference is negligible.

The Fourier transform of $k\chi(k)$ shows peaks corresponding to near neighbors of the Rh atom (Figure 1b). The largest peak at 1.5 Å can be identified with the oxygens of the acetate ligands and the second peak mainly with the neighboring Rh atom with possible superposition of the axial nitrogens. Peaks farther away are from more distant neighbors. The Rh peak of the Fourier transform was inverted to extract its phase. The Rh–Rh signal extends to 20 $Å^{-1}$. Below 10 $Å^{-1}$ the Rh–Rh signal was complicated by backscattering from lighter atomic ligands. Analysis of the phase from 10 to 17 $Å^{-1}$ gives definitive Rh–Rh distances (Table I).

For comparison, the simple compounds $[Rh_2(O_2CR)_4 \cdot 2MeOH]$ (R = CH_3 or n-C_3H_7) were also examined. Only for the latter case were figures obtained; excessive noise, the origin of which is not yet clear, made data for the acetate dimer unanalyzable.

The crystal structure of $[Rh_2(O_2CC_3H_7)_4 \cdot 2MeOH]$ has not been determined; the value we obtain, 2.369 ± 0.005 Å, is one of the shortest Rh–Rh bond lengths observed[21] in the carboxylate series and is consistent with the diminuition of this distance upon change in the R group. For example, $Rh_2(O_2CR)_4 \cdot 2H_2O$ where R = CH_3 has Rh–Rh = 2.3855 Å and R = CMe_3 has Rh–Rh = 2.371 Å. No data are available for a comparison of diaquo and dialcohol adducts for the same R group. The Rh–Rh distance in the $[Rh_2(O_2CR)_4L_2]$ species, in fact, changes only slightly upon variation of R and L for those structures determined but a further decrease might be expected for $[Rh_2(O_2CC_3H_7)_4 \cdot 2H_2O]$; this point is under investigation.

For the nucleoside adducts, examination of the data in Figure 1a confirms the structural similarity within the series. No significant difference is found in comparison to the standard used, $[Rh_2(O_2CCH_3)_4(caffeine)_2]$[10] and, indeed, $[Rh_2(O_2CCH_3)_4 \cdot py_2]$ where r(Rh–Rh) = 2.3963 Å,[21] although the related bis(theophylline) adduct has r(Rh–Rh) = 2.412 Å. No simple correlation exists between Rh–Rh lengths and basicity of the nitrogen donor atom.

The interference between the oxygen and rhodium shells obviously differs between the 8-bromoadenosine adduct and all the others. The beating node at about 8 $Å^{-1}$ has a double hump in the spectra of all other complexes and the relative height of the first and second Fourier transform peaks is reversed. The interpretation of these features is not immediately obvious. Furthermore, simply Fourier filtering the oxygen peak is not possible because rhodium's backscattering amplitude has a dip at 7 $Å^{-1}$ that produces a wing on the lower side of its main peak which merges with the oxygen peak. Therefore we used curve-fitting to analyze the two-shell spectra.

For the *fit analysis* the Fourier-filtered data were fit to eq 1 with $A_i(k) = 1$. Initially, the caffeine adduct was fitted to obtain empirical phase shifts consistent with the known interatomic distances. The empirical phase shifts were derived from theoretical ones by adding a constant and a linear term

$$\alpha(k) = \delta_A(k) + \delta_B(k) + \alpha_0 + a_1 k$$

where δ_A and δ_B are calculated phase shifts for the absorbing and backscattering atom.[22] E_0 was fixed at the inflection point of the absorption edge. Values of a_0 and a_1 for both Rh–Rh phase and Rh–O phase were determined by the best fit assuming bond lengths known from X-ray crystallography: $a_0 = -0.65$, $a_1 = 0.0642$ Å for oxygen, and $a_0 = 1.135$, $a_1 = 0.040$ Å for rhodium.

(21) Felthouse, T. R. *Prog. Inorg. Chem.* **1982**, *29*, 73.
(22) Teo, B. K.; Lee, P. A. *J. Am. Chem. Soc.*, **1979**, *101*, 2815.

Table I. Values Obtained from Analysis of Rh Edge EXAFS Spectra

compd	phase analysis r(Rh–Rh), Å	curve fit analysis r(Rh–O), Å	σ^2(Rh–O) × 10^3, Å^2	r(Rh–Rh), Å	σ^2(Rh–Rh) × 10^3, Å^2	GOF
$[Rh_2Ac_4(caffeine)_2]$	2.395 (1)[a]	2.036	4.29	2.395	1.88	0.43
$[Rh_2Ac_4(adenosine)]\cdot H_2O$	2.392 (3)	2.035	3.92	2.388	1.84	0.52
$[Rh_2Ac_4(cordycepin)]\cdot H_2O$	2.397 (5)	2.040	5.32	2.394	2.02	0.68
$[Rh_2Ac_4(ara\text{-}A)]\cdot H_2O$	2.397 (3)	2.044	4.43	2.398	1.72	1.78
$[Rh_2Bu_4\cdot 2MeOH]$	2.369 (5)	2.035	3.78	2.364	1.75	1.77
$[Rh_2Ac_4(8\text{-}Br\text{-}adenosine)]\cdot H_2O$	2.394 (11)	2.020	2.17	2.379	2.51	1.28
uncertainty[b]		0.011	1.40	0.011	1.15	

[a] Figures in parentheses represent the estimated error in the least significant digits based on the uncertainty of the phase analysis plus the uncertainty of the value in the standard. [b] Average variation of fit values needed to increase GOF by 1 while allowing other parameters to be adjusted for the best fit.

Varying σ^2 and η allows sufficient modification of the total amplitude to compensate for inadequacies in the theoretical amplitudes $|f(k,\pi)|$. Thus the values of η and σ^2 may be inexact though relative values of σ^2 within the series should be meaningful. The mean free path was modeled by $\lambda = k/\eta$ where η was determined to be 1.97 by fitting the caffeine complex spectrum and fixed at this value for the other compounds. All fits were to $k\chi(k)$. The goodness-of-fit (GOF) measure used was the residual sum of squares between fit and data divided by an error estimate. The error estimate was 0.1 except for the nodal region 7.5–10 Å^{-1} where it was set at 0.02 in order to improve the fit to the node. A third shell for the axial N or O at about 2.3 Å could not be fit because the GOF proved to be an erratic function of the bond length. This shell is probably negligible because of the much stronger signal from the four O atoms and the Rh atom.

The fitting results (Table I) reveal the source of the spectral differences of the 8-bromoadenosine species: the disorder parameter, σ^2, of the Rh–O bond length decreases while that of the Rh–Rh bond length increases. The fits (see Figure 2) also indicate shorter Rh–Rh and Rh–O bond lengths, though these differences are barely significant and the Rh–Rh distance decrease is not confirmed by the phase analysis. The decrease in disorder of the Rh–O distance may derive from either a reduction in thermal motion or less variability among the four bond lengths. These results suggest a markedly different complexation of Rhodium carboxylate to 8-bromoadenosine than to adenosine which is discussed below.

The curve fit method gives values for r(Rh–Rh) which generally agree with those of the phase difference analysis. The many more variable parameters used in curve fitting probably introduce more uncertainty in the results and we therefore have greater confidence in the Rh–Rh distances of the phase analysis.

One unresolved question is the ambiguity of the possible Rh binding site to adenosine. For adenosine binding, the sugur blocks N_9 leaving as possible binding sites N_7, N_1, or the amine N_6. Indirect spectroscopic evidence suggests that N_7 binding is likely.[9,10] The rhodium edge spectra show no features which can obviously be assigned to structure outside the rhodium carboxylate complex. In particular, a contribution from Br backscattering is absent in the 8-bromoadenosine adduct's spectrum. If binding were at N_7, a Br-Rh distance near 3.6 Å would be observable. Analysis of the Br edge spectrum confirms the absence of a Rh–Br contribution and shows other features related to the nucleoside structure.

Bromine-Edge Spectra. The spectra and their Fourier transforms are shown in Figure 3. As the exact crystal structure of 8-bromoadenosine is known[23] its spectrum can serve as a calibration for the Br edge spectrum of its rhodium acetate complex. 8-Bromoadenosine is in the syn conformation and the peaks of the Fourier transform of its spectrum correlate with known interatomic distances. The peak 1 (Figure 3b) is identified with C_8 at 1.855 Å, peak 2 with N_7 and N_9 at 2.814 and 2.860 Å and peak 3 with C_4 and C_5 backscattering at 3.946 and 3.941 Å. Peak 5 is mainly C_6 and N_3 with possibly some contributions from atoms on the ribose moiety. Peak 4 may be identified with the 2′ oxygen, the C_2' carbon and the heterocyclic oxygen, at 4.442, 4.475, and 4.258 Å, respectively. This peak, as can be seen by comparison of the room- and low-temperature spectra, is more sensitive to temperature as would be expected for atoms on the sugar which are more susceptible to thermal motion than those on the purine. If only one atom were at this distance it is unlikely that it would be possible to observe this peak. Therefore, the syn conformation of the sugar with respect to the purine ring can be recognized by the existence of this peak.

In the rhodium acetate adduct, peaks 1, 2, 3, and 5 are identifiable with the same peaks in the free nucleoside. Peak 4,

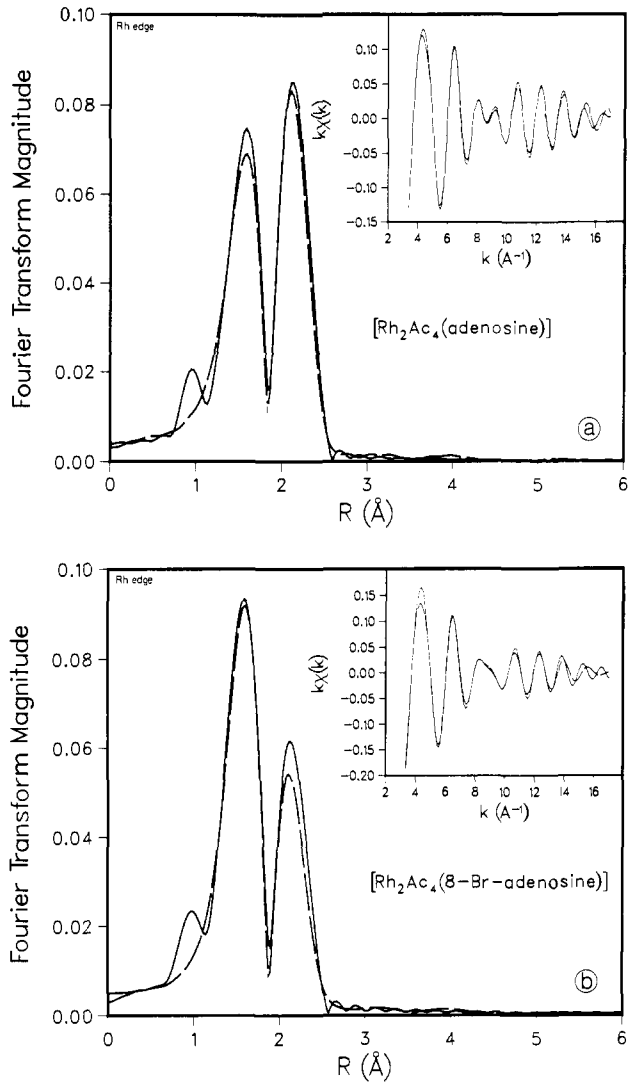

Figure 2. Rh-edge spectra and transforms filtered between 1 and 2.5 Å. The solid lines are the data and the dashed lines are the fit. The R-space curves are the transforms of the spectra shown in the insets between 2.5 and 16 Å^{-1}. The side lobe below 1 Å is an artifact from truncation of the data. (a) $[Rh_2Ac_4(adenosine)]\cdot H_2O$; (b) $[Rh_2Ac_4(8\text{-}Br\text{-}adenosine)]\cdot H_2O$.

(23) Tavale, S. S.; Sobell, H. M. *J. Mol. Biol.* **1978**, *48*, 109.

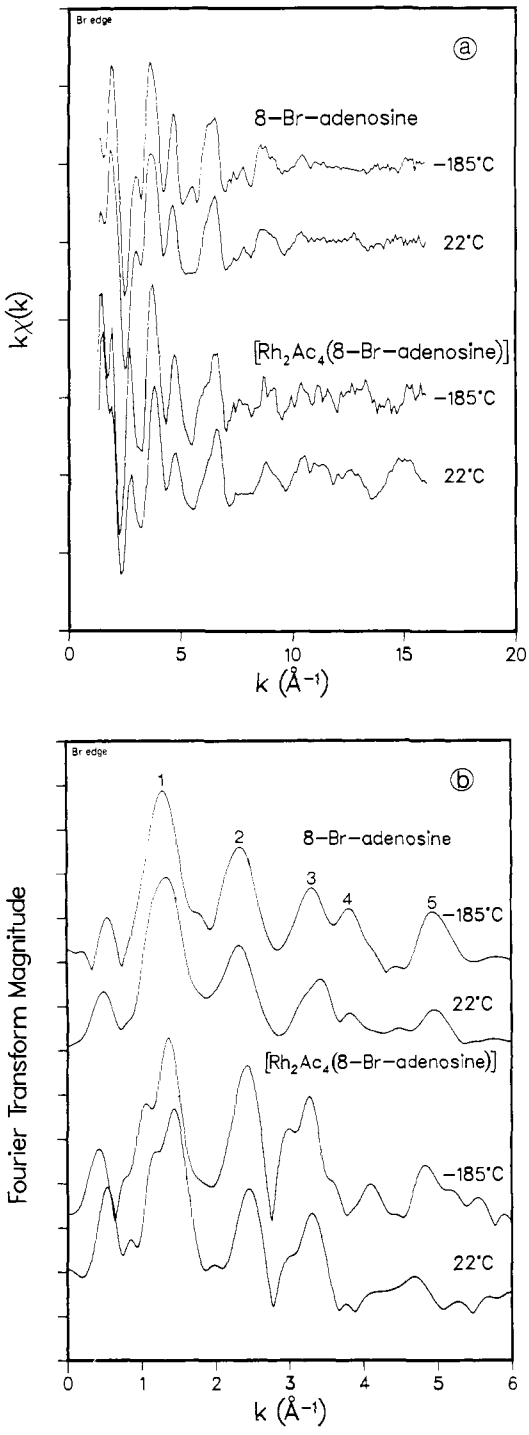

Figure 3. (a) EXAFS spectra of the Br-edge of 8-bromoadenosine and $[Rh_2Ac_4(8\text{-Br-adenosine})]$ at −185 and 22 °C. (b) Fourier transforms of the spectra of a. Peaks 1, 2, 3, and 5 are identified with atoms of the adenine where peak 4 arises from the nucleoside moiety. The change of peak 4 in the rhodium acetate complex indicates a syn to anti conformational change. Transforms are of $k\chi(k)$ over a range of 2.47–16 Å^{-1} with a 10% Gaussian window.

however, is considerably reduced and a shoulder appears on the lower side of peak 3 at 3 Å. The absence of peak 4 implies a movement of the sugar, probably to the anti conformation. The movement can be calculated to bring several atoms, e.g., heterocyclic oxygen, into conjuction around 3–3.7 Å which could produce this shoulder. This argument, coupled with the absence of a strong Br peak in the Rh spectrum (Figure 1b), does not permit us to identify this shoulder as being due to rhodium backscattering. This strongly implies binding at N_1, as the alternative N_7 binding should give an observable Rh–Br distance of approximately 3.6 Å. The arguments allow us to assign the structure of this complex as N_1–bound with the sugar in the anti conformation (Figure 4).

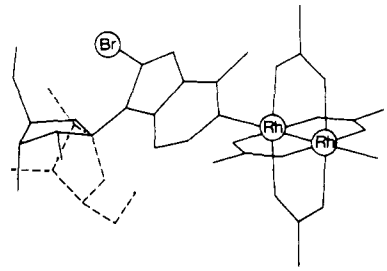

Figure 4. Possible structure of Rh_2Ac_4 bound at N_1 to 8-bromoadenosine in the anti conformation. The dashed lines show the nucleoside in the syn conformation.

Conclusion

These results still leave in doubt an unequivocal assignment of the binding sites in the non-brominated adenosine species. Bromine substitution may favor N_1 over N_7 binding by steric or electronegative factors and the H-bonding factors referred to may still be important. In the case of the Rh-edge EXAFS spectra, the non-brominated acetate complexes are virtually identical (Figure 1). This implies that differences due to different purine structure, other than the binding atom, are not discernible. However, it is of interest that the substitution of bromine produces alterations in the beating node at 9 Å^{-1} which translates into a change in the relative amplitudes of the first and second peaks (Figures 1b, 2a, and 2b). The similarity in the Rh-edge EXAFS spectra of the caffeine adduct and the non-brominated adenine nucleoside adducts indicate a very similar environment. As the caffeine adduct is known to be a 2:1 species with N_9 as the monodentate binding site, this type of environment could be achieved for adenosine by bidentate bridging using both N_1 and N_7. This is not possible for the brominated complex, which may be assumed to have a solvent molecule (e.g., H_2O) in the other axial position. The spectrum of the butyrate complex differs from that of caffeine mainly because of changes in r(Rh–Rh).

Although the EXAFS of the brominated derivative did not directly identify the rhodium atom, its absence suggested assigning the binding site to N_1. The structure of the Fourier transforms clearly shows evidence of a syn to anti conformation change. The free adenosine is in the anti conformation whereas bromination induces crystallization in the syn conformation. Metalation of 8-bromoadenosine reverses the conformation to anti. This work emphasizes the utility of EXAFS in structural problems of this type and extension to other brominated purines and pyrimidines should be of interest. The results also confirm that, as expected, the antibiotics behave like adenosine in their binding to metals. The complexes are the first reported of adenine-based nucleosides with biological activity and these complexes are currently being evaluated.

Acknowledgment. We thank A. J. Seary for computer programs used in data collection and analysis and the staff of the Stanford Synchrotron Radiation Laboratory for technical assistance. We are also grateful to the Chemistry Department at Simon Fraser University where this work began. The research was partially funded by a grant from the Natural Sciences and Engineering Research Council of Canada. The Stanford Synchrotron Radiation Laboratory is supported by the Department of Energy through the Office of Basic Energy Sciences and the National Institutes of Health through the Biotechnology Resource Program in the Division of Research Resources.

Registry No. $[Rh_2Ac_4(\text{adenosine})]\cdot H_2O$, 76601-59-7; $[Rh_2Ac_4(\text{cordycepin})]\cdot H_2O$, 93473-57-5; $[Rh_2Ac_4(\text{ara-A})]\cdot H_2O$, 76601-59-7; $[Rh_2Ac_4(8\text{-Br-adenosine}]\cdot H_2O$, 93473-58-6; $[Rh_2Ac_4(\text{caffeine})_2]$, 74472-61-0; $[Rh_2Bu_4\cdot 2MeOH]$, 93473-59-7.